

First principles study structural and magnetic properties of Mn doped MgO

Y. Benkrima^{a,*}, A. Souigat^a, M.E. Soudani^b, Z. Korichi^a, H. Bouguettaia^c

^a Department of Exact Sciences, ENS Ouargla, Algeria.

^b Laboratory of New and Renewable Energy in Arid and Saharan Zones (LENREZA), Ouargla University, Algeria.

^c Department of Physics, Faculty of Mathematics and Matter Sciences, Kasdi Merbah University, P.O. Box 511, 30000 Ouargla, Algeria.

The structure, electronic and magnetic properties of the MgO bulk of (1x2x2) and (1x1x1) atoms for the B4 wurtzite phase, doped by Manganese Mn have been studied. Accordingly, the Mn atom location in the far and near spots was taken into account, as well as recognizing the magnetic interaction between both spots. Such initiative was provided thanks to the use of the density function theorem (DFT). As for the energy gap of the semiconductor MgO, it was calculated by the linearly increasing planar method, and by the local density approximation (LDA), not to mention the generalized gradient approximation (CGA). It is found that the calculated results agree well with other theoretical and experimental findings. Whereas, the energy gap and the total magnetic torque have been recorded for the Mn doped MgO in the (1x2x2) super Celle. Therefore, our given results have shown that the use of the classification-generalized approximation could enable us to provide more precise results of the d orbital composites, and they also added new properties to the new compound.

(Received June 15, 2022; Accepted October 14, 2022)

Keywords: Ab-initio study, MgO, Mn doped, Structural properties, Electronic properties, Magnetic properties

1. Introduction

Magnesium monoxide, MgO, is a group II-V semiconductor material with a large energy gap of about 3.4 to 7.8 eV [1]. Alloys of this material show an increased amount of radiation in the vicinity of UV rays, specifically in the [150, 400] nm field. Nano-materials are generally used in various applications, such as, photovoltaic, electrochemical, mechanical and sensor[2]. In addition, for smart phones, satellites, and optical fibre transmission systems, as well as incorporating them into other advanced technologies such as laser diode manufacturing, magnetic detectors...etc. This technology has changed our lives, as we are obliged to use it constantly nowadays. The properties of semiconductors change if metal impurities are added such as energy gap, density of states, magnetic properties...etc.

Group II-VI or II-V semiconductor materials dotted with transition metals can be used in many applications, especially with regard to the remarkable magnetic properties when studying and using semiconductor compounds. Besides the well-known term Dilute Magnetic Semiconductors (DMS's) for the above semiconductors, these semiconductors are very likely to be among the core structures of Spintronic devices [3].

Recently, (DMSs) devices studying have attracted the attention of many researchers worldwide; and that is due to the Two Compounds of Spin and Charge being used as magneto-optical transmission devices and that of electromagnetic ones as well [4-7].

In such dilute magnetic semiconductors, one of the magnetic impurities replaces the cations; moreover, the process of replacing cations could lead to the addition of new magnetic

*Corresponding author: benkrimayamina@gmail.com

<https://doi.org/10.15251/JOR.2022.185.681>

properties to the very semiconductors. Yet, this process should not be able to interfere with the (DMSs) optoelectronic properties [8]. Adopted in the study of the basic properties of (DMSs) based on the compound MgO, which was recently investigated by Mathon and Amarchi [9]; a significant increase in the magnetic resistance (MR) of magnetic tunnel connections outside of MgO was expected, based on first-principles calculations. The theoretical predictions are then confronted to experimental studies for confirmation.

These studies are those of the S.S.P. Parkin et al and S.Yuasa and others [10], where MgO was magnetically synthesized by dilute magnetic doping. It can also be a good spin filter [11-12] in addition to the effect of creating a wide magnetic field [13]. Despite efforts made in both theoretical and applied studies to understand the compound, and the magnetic property within MgO; it remains the focus of current intensive studies. Lately, studies of MgO compounds saturated with transition metals have brought researchers' attention to understanding the acquired ferromagnetic nature of MgO, which will also be addressed using first-principles calculations in this work.

Firstly, MgO is doped with two Mn atoms. Next, highlight new structural properties of the compound, and then find the electronic and magnetic properties of the novel formulations of Mn:MgO; where it is better to use first principles based on density function theory (DFT) initially to predict the effect of doping actions on oxides before conducting experiment and real work. To this end, we generated ferromagnetic (FM) and anti-ferromagnetic (AFM) coupling only so that we could see the structural, magnetic and electronic properties affected by the above process. In addition, it is believed that our findings can bring countless seekers of theoretical knowledge about the effect of impurities. Conclusively, we seek to fully demonstrate the newly obtained new properties of Mn:MgO. The main objective of this study is to provide principles and predictions about how to synthesize new magnetic materials from semiconductors and know their properties. To clarify this idea, we relied in this work on the density function theory.

2. Theoretical method of calculation

At this point, we have performed simulations by using a computational program called Spanish Initiative for Electronic Simulations with thousands of atoms (SIESTA). The latter is based on density functional theory [14]. The whole system is optimized by following all the basic steps like network cutting, k point, network optimization...etc. In addition, in order to obtain suitable results, all atoms must remain absolutely fixed in their positions while the optimization procedure is performed. Moreover, for exchange and correlation potentials, the generalized gradient approximation (GGA) of Perdew– Burke–Ernzerhof is utilized herein [15] and local density approximation [16]. Core electrons are modelled with Troullier–Martins' norm-conserving pseudo potentials [17]. The valence electrons functions are expanded in double zeta polarized basis set [18-19] of localized orbital, and the real space grid is set to be 350 Ry. Until the Hellmann–Feynman forces acting on all components of each atom are smaller than $0.01 \text{ eV}\text{\AA}^{-1}$ and the structure is still stable. This process yielded a fully optimized MgO nanostructure which contained 2 Mg and 2 O atoms.

3. Results and Discussion

3.1. Structural Properties

The network constants for MgO have been investigated many times, and this process has been conducted over several decades [20]. The primary cell structure of the stable magnesium oxide MgO is from the [B4] wurtzite phase. This compact hexagon characterizes group P6₃mc and grid constants are estimated at $a=b= 3.283 \text{ \AA}$, $c= 5.095 \text{ \AA}$, $\alpha=90.03^\circ$, $\beta=90.037^\circ$, $\gamma=119.90^\circ$ [21]. In the current study, our calculations are based on the SIESTA program, through which we will calculate the initial cell constants for MgO. The results are displayed in Table 1.

Table 1. Primary cell constants of MgO oxide and its comparison to theoretical and practical results.

	a (Å)	c (Å)	μ (Å)	c/a
Present work	3.327	5.025	1.0117	1.5103
GGA	3.288	5.004	1.2205	1.5219
Theoretical works	3.3088 ²²	5.0748 ²²	0.38608 ²²	/
GGA	3.281 ²³	5.136 ²³	0.393 ²³	/
	3.3105 ²⁴	5.12363 ²⁴	0.3915 ²⁴	1.5476 ²⁴
Theoretical works	3.25284 ²²	5.0278 ²²	0.3916 ²²	/
LDA	3.322 ²⁰	/	0.3916 ²⁰	/
	3.2493 ²⁴	5.2778 ²⁴	0.39171 ²⁴	1.546 ²⁰
	3.32 ²¹	5.056 ²¹	0.386 ²¹	1.5473 ²⁴
	3.169 ²⁵	5.175 ²⁵	0.3750 ²⁵	1.565 ²¹
		/	/	1.5366 ²⁵
				1.5296 ²⁶
Experimental work	3.283 ²¹	5.095 ²¹	0.388 ²¹	1.552 ²¹

Based on the density function theory (DFT) and SIESTA software, we were able to calculate the initial cell constants, where the value 3.327 Å for the constant a, and 5.025 Å, for the constant c were recorded. Considering that the structure is hexagonal, thanks to which we get equal values for the constants a and b. These results are largely consistent with the theoretical and applied results mentioned above in Table1 [21-26]. Moreover, the error rate in the results of our work was calculated and compared to the obtained experimental results. An estimated error rate of 1.34% for the constant a, and 1.37% for the constant c were obtained using the GGA approximation.

3.2. Electronic Properties

3.2.1. Bands Structures

The specific berillion region is the first structure in the study of the electronic properties of the material body. The diagram below represented in Figure 2 shows the results of the electronic study of the berillion region associated with the hexagonal phase of MgO, which will then be generalized to all parts of the oxide. Both the density functional theory (DFT) and the Generalized Gradient Approximation GGA have been used to determine the magnesium oxide energy gap MgO. This method, being the most recommended one, also specializes in studying electronic structures of materials, for example, the energy ranges of magnesium oxide MgO. The latter is computed for the previously calculated network constant.

$$(a = 3.327 \text{ \AA}, c = 5.025 \text{ \AA}, \alpha = 90.03^\circ, \beta = 90.037^\circ, \gamma = 119.90^\circ)$$

The structure of the energy bands for the MgO compound shown in Fig. 1 was calculated.

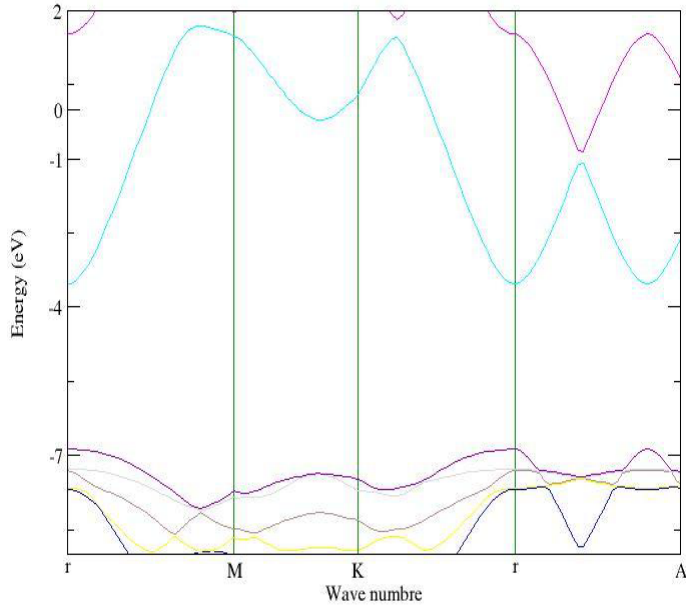


Fig. 1. The structure of oxide energy bands MgO phase wurtzite in GGA approximation.

According to the previous graph, the highest peak in the valence band and the lowest in the conduction band are placed practically on the same line as the point τ , showing that MgO has a direct gap of 3.27 eV using GGA approximation and 3.18 eV using an LDA approximation. The energy gap value based on both approximations GGA and LDA was computed; and its comparison with other theoretical results are shown in Table 2.

Table 2. The energy gap and its comparison with other experimental and theoretical values.

Energy gap (eV)		approximation used
LDA	GGA	
3.18	3.27	Our results
3.607 ²²	3.891 ²²	
/ 4.968 ²⁸ 5.05 ³⁰ /	4.408 ²⁷ 4.431 ²⁸ 4.45 ²⁹ 5.42 ²⁹	Other results

It could be noticed that the value of the energy gap was close to the theoretical results shown in Table 2, while the calculated results for the structure of the energy bands based on the approximation GGA were somewhat lower than the experimental results. This indicates that this particular numerical method does not provide results close to reality, despite the convergence of the two energy gap values calculated using different approximations GGA and LDA. Compared to the experimental results, although if a local density approximation LDA is used, the value of the energy bands will always be less than the experimental value as presented in citation [23]. As is generally known, both approximations GGA and LDA reduce the computed energy gap value to the experimental value; hence, the computed value remains only as an estimate of the actual values of the energy gap [31].

3.3. Magnetic properties

To know and study the magnetic properties of the MgO compound, a dual primary structure was taken by taking the cell ($1 \times 2 \times 2$), or in the sense two cells in the direction of the y-axis was taken. Similarly in the direction of the z-axis, and one cell in the direction of the x-axis. In this study, we seek to effect the grafting of MgO with two Mn atoms. Since MgO is a non-magnetic compound, we add two atoms of the element Mn that has magnetic properties. Thus, we will search for the effect of doping on the magnetic properties of the MgO compound. When we graft the compound MgO with two atoms of magnesium Mn, we will study again the new compound obtained, which is Mn:MgO in terms of structural, magnetic and electronic properties as well.

3.3.1. Structural Properties

The pellets in blue represent magnesium Mg, the red ones represent oxygen O, whereas the purple ones represent manganese.

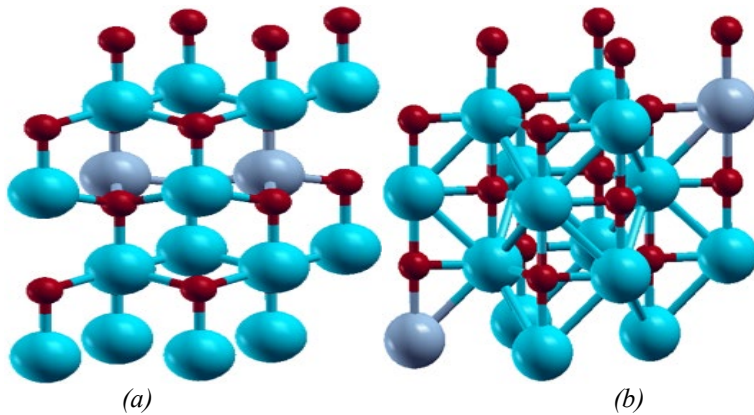


Fig. 2. The crystal structure of the composite Mn:MgO in (a) convergence and (b) Spacing.

After reaching the stability of the compound and the relaxation of its atoms, we worked on changing the positions of the two magnesium atoms, by making them close sometimes and apart other times. The magnetic moment of each of the atoms Mn_1 , Mn_2 and O was then calculated, as well as the length of the bonds between (Mn - O) and (Mn - Mn) in the cases of convergence and divergence of the two magnesium atoms inside the compound Mn:MgO. These calculations were done using both approximations (GGA) and (LDA). The results are shown in Table 3.

Table 3. Magnetic moments of Mn_1 , Mn_2 and O atoms, and the new bond lengths between (Mn - Mn) and (Mn - O).

Approximation	Statue	Distance Mn - O Å	Distance Mn-Mn Å	Magnetic moment Mn_1 μ_B	Magnetic moment Mn_2 μ_B	Magnetic moment O μ_B
GGA	Convergence	2.030	3.338	2.6983	-2.6983	0.0039
	Spacing	2.1814	10.237	2.6983	2.6983	0.0038
LDA	Convergence	2.068	3.366	2.6988	-2.6988	0.0038
	Spacing	2.197	10.382	2.6988	2.6988	0.0056

Table 3 represents the values of the bond length between (O - Mn) and (Mn - Mn), as well as the magnetic moments of Mn1, Mn2 and O atoms. The table shows that almost all magnetic moments of manganese atoms are between (2.6-2.7) μ_B , and this is due to the main reason, which is the effect of electrons in the "d" terminal of Mn atoms. Furthermore, it is found in the O atoms of the Mn:MgO compound; positive values of the magnetic moment appeared, as they appeared in both cases of convergence and divergence of the magnesium atoms. So far, it has been found that the magnetic moments were weak and were estimated in the range (0.003-0.005) μ_B . As for, the bond length recorded in D (Mn-Mn) in closely spaced manganese atoms, it is actually on the order of 3.338 Å, and in the spacing statue is 10.237 Å. This was in the case of using (GGA) approximation, whereas, for the case (LDA) approximation, the recorded bond length was 3.366 Å when the manganese atoms were close and 10.382 Å when the atoms were a part. The nature of the magnetic coupling of the compound Mn:MgO is summarised in Table 4.

Table 4. Nature of the magnetic mating in both convergence and Spacing of the Mn atoms using GGA and LDA approximation.

Approximation	Status	Anti-ferromagnetic AFM(eV)	Ferromagnetic FM (eV)	Difference between energies spin polarization energy	Mating Nature
GGA	convergence	-6191.848	-6191.8806	-0.032	Anti-ferromagnetic Anti-Ferromagnetic
	Spacing	-6191.8474	-6191.826	-0.021	
LDA	convergence	-6190.513	-6190.5484	-0.035	Anti-ferromagnetic Anti-ferromagnetic
	Spacing	-6190.4878	-6190.458	-0.0293	

Table 4 presents the ferromagnetic energy along with manganese Mn_{FM} , and the anti-ferromagnetic energy of MgO_{AFM} . In addition, the energy of the rotational polarization difference $\Delta E(AFM-FM)$, not to mention the display of the nature of magnetic coupling occurring amid the Mn atoms of the Mn:MgO complex in the structure from the figure (1x2x2). We have noticed that the spin polarization energy is the calculated energy difference between the anti-ferromagnetic energy and the ferromagnetic energy, which was a positive result in both approximations used and in the cases of convergence and divergence. This indicates that the ferromagnetic state is the most stable compared to the ferromagnetic for Mn:MgO. Conclusively, we tend to say that Mn:MgO tends to be a non-magnetic compound.

3.3.2. Electronic properties

In this section, energy ranges and state densities of MgO will be discussed before and after doping for both cases of convergence and divergence of Mn atoms. All calculations were performed using generalized gradient approximation GGA for the selected cell (1×2×2) and the fig. 3 shows that.

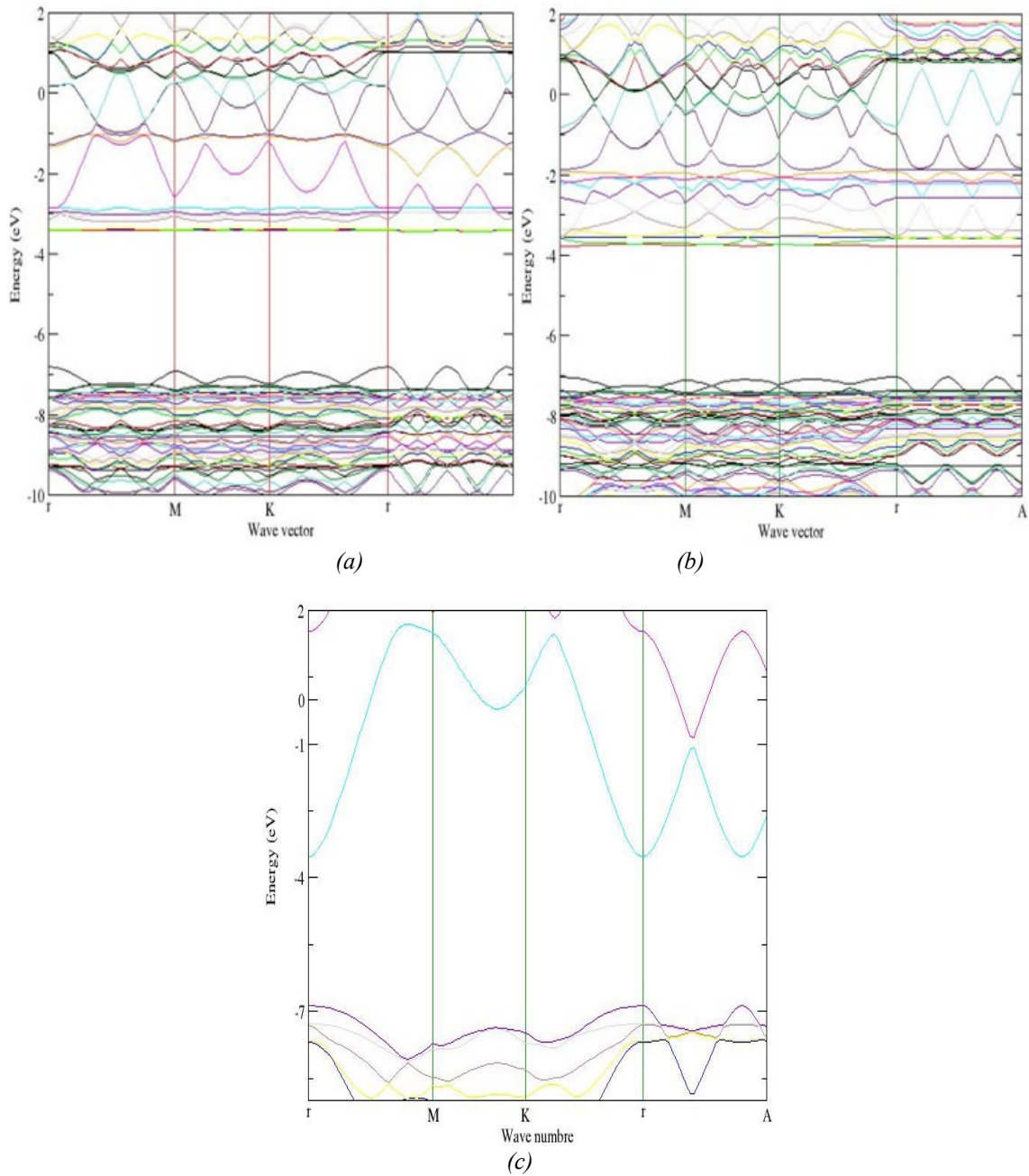


Fig. 3. The structure of energy bands of the Mn:MgO, (a) in Spacing, (b) in convergence. (c) MgO bulk.

Based on the graph in Figure 3, and by calculating the energy gap band that was visible through the highest peak of the valence band, and those at the bottom of the conduction band; the obtained value was approximately equal to 3.2 eV in manganese atoms in the convergence or divergence cases. It is also noticed that the value of the energy gap before the process of doping the MgO bulk with two manganese atoms was greater than that recorded after doping with an estimated difference of 0.1 eV.

3.3.3. The density of states (DOS)

To comprehend the band structure and magnetic bond structure of the Mn doped MgO and determine the total density of states (TDOS) in both convergence and divergence states in the (1×2×2) structure; it is indispensable to clarify the density of states before and after doping in both cases.

3.3.3.1. Convergence status

3.3.3.2. Spacing status

Figures 4 and 5 compare total spin polarized in the case of MgO in bulk state with the total spin polarized density of states for the AFM states doped with Mn atoms in convergence and divergent states. The total spin polarized of states in the case of doping MgO with two Mn in convergence seems to appear symmetrically with that of MgO in bulk. This was not seen in the other case, since the ups and downs of the total spin polarized near the Fermi region (at energy 0 eV) showed symmetry as in figure 4. Hence, in the case of the MgO compound doping with Mn atoms in their convergence state, we find that the Mn:MgO compound did not add anything new to the electronic distribution of the MgO compound. In addition, for the case of doping of MgO with two divergent Mn atoms, the compound shows a diversity of intensity values of states recorded near the Fermi proximal region (at energy 0 eV) as in Fig. 5. Moreover, the new compound demonstrates new characteristics that MgO did not have previously.

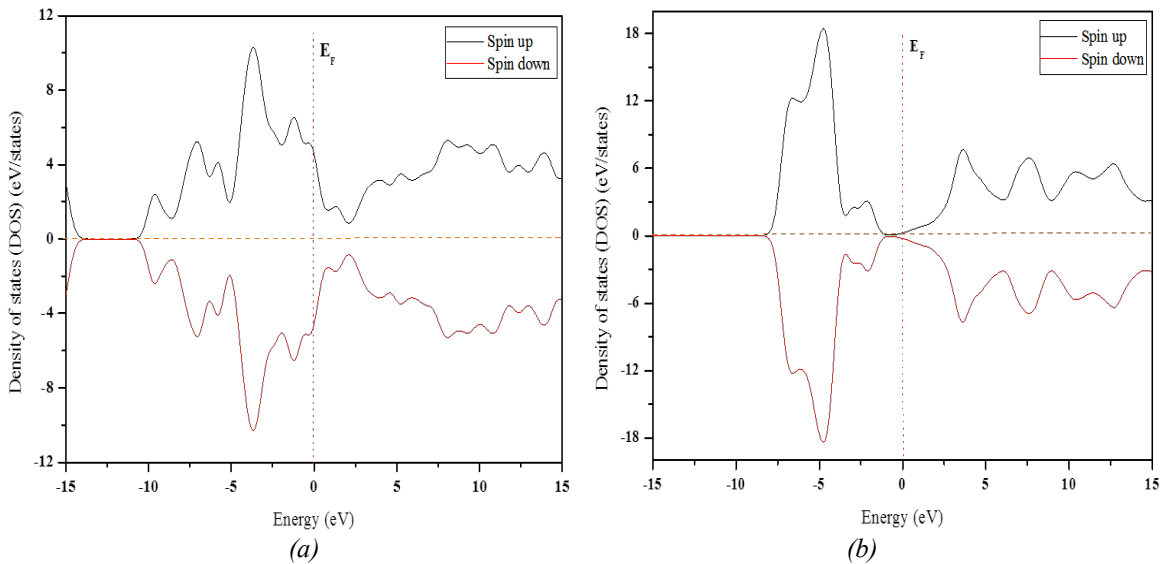


Fig. 4. Spin polarization density of the Mn:MgO, (a) before doping, (b) after doping in convergence state.

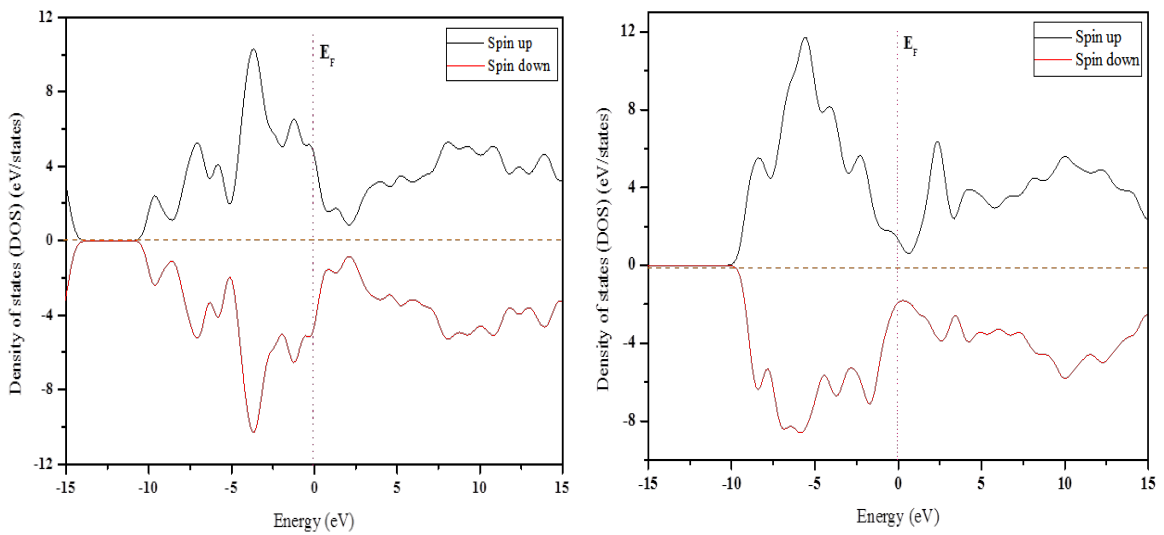


Fig. 5. Spin polarization density of the Mn:MgO, (a) before doping ,(b) after doping in Spacing state.

In this case, we clearly highlight the fact that it acquires magnetic properties that enable it to be incorporated into electronic structures for magnetic use. The values for prominent total spin polarized near the Fermi region are originally due to the “d” orbital of Mn. Thus, we conclude, that the manganese element, Mn, contributed to the formation of the electron density of the new compound Mn:MgO

4. Conclusions

In order to clarify the ferromagnetic potentials of the Mn:MgO composite, we systematically studied the electronic structure, the electronic and the magnetic properties as well for the (B4) wurtzite stable phase. The first principles have been calculated using GGA and LDA approximations, as both are under the realm of the Density Function Theorem. The results showed that the existence of manganese as an impurity in-phase (B4) was in fact, an addition of a full magnetic torque, which was in the spacing state of both of manganese atoms Mn. Furthermore, the Mn impurity does not mainly affect the grid constants of the MgO composite. However, the latter adds up its touch at the energy gap, where variance appears therein, and the Mn:MgO composite is a system that is preferable of anti-ferromagnetic characterizations; that if the impurity is to be found with two approximate manganese atoms, Mn: MgO systems favors anti-ferromagnetism as the fundamental stable state. The observed highly spin polarized conduction carriers indicate that Mn:MgO in wurtzite phase materials have a potential for polarized spin current applications and other spintronic devices.

References

- [1] A. M. Ghaleba, R.A.Munef, S.F. Mohammed, Journal of Ovonic Research 18, 11 (2022);
<https://doi.org/10.15251/JOR.2022.181.11>
- [2] G.M. Whitesides, B. Grzyboski, Science 295, 2418 (2002);
<https://doi.org/10.1126/science.1070821>
- [3] D. Benjamin, O. David, J. Pauzauskie, H. Rongrui, P. Yang, Angew. ChemInt 45, 423 (2006).
- [4] H. Ohno, Science 281, 951 (1998); <https://doi.org/10.1126/science.281.5379.951>
- [5] T. Dietl, H. Ohno, F. Matsukura, J. Cibert, D. Ferrand, Science 287, 1019 (2000);
<https://doi.org/10.1126/science.287.5455.1019>
- [6] Z.W. Pai, Z.R. Dai, Z.L. Wang, Science 281, 1947 (2001).
- [7] M.H. Huang, S. Mao, H. Feick, H.Q. Yan, Y.Y. Wu, H. Kind, E. Weber, R. Russo, P.D. Yang, Science 292, 1897 (2001); <https://doi.org/10.1126/science.1060367>
- [8] H. Ohno, Science 281, 951 (1998); <https://doi.org/10.1126/science.281.5379.951>
- [9] J. Mathon, A. Umerski, Phys Rev B 63, 220403 (2001);
<https://doi.org/10.1103/PhysRevB.63.220403>
- [10] S.S.P. Parkin, C. Kaiser, A. Panchula, P.M. Rice, B. Hughes, M. Samant, S.H. Yang, Nature Mater 3, 862 (2004); <https://doi.org/10.1038/nmat1256>
- [11] S. Yuasa, T. Nagahama, A. Fukushima, Y. Suzuki, K. Ando, Nature Mater 3, 868 (2004);
<https://doi.org/10.1038/nmat1257>
- [12] I. Zutic, J. Fabian, D.S. Sarma, Rev Mod Phys 76, 323 (2004);
<https://doi.org/10.1103/RevModPhys.76.323>
- [13] L. Esaki, P.J. Stiles, S. Von Molnar, Phys Rev Lett 19, 852 (1967);
<https://doi.org/10.1103/PhysRevLett.19.852>
- [14] P. Hohenberg, W. Kohn, Phys Rev B136, 864 (1964);
<https://doi.org/10.1103/PhysRev.136.B864>
- [15] J.P. Perdew, K. Burke, J Phys RevLett 77, 865 (19963).
- [16] A.D. Becke, E.R. Johnson, J. Chem. Phys 124, 221101 (2006);

<https://doi.org/10.1063/1.2213970>

- [17] N. Trouillier, J.L. Martins, J Phys Rev B 43, 1993 (1991);
<https://doi.org/10.1103/PhysRevB.43.1993>
- [18] J. Junquera, O. Paz, D.S. Portal, E. Artacho, J Phys Rev B 64, 235111 (2001);
<https://doi.org/10.1103/PhysRevB.64.235111>
- [19] C. Shen, J. Wang, Z. Tang, H. Wang, H. Lian, J. Zhang, ElectrochimActa 54, 3490 (2009);
<https://doi.org/10.1016/j.electacta.2009.01.014>
- [20] A. Schleife, F. Fuchs, J. Furthmüller, F. Bechstedt, Phys Rev B 73, 245212 (2006).
- [21] M. Toporkov, D.O. Demchenko, Z. Zolnai, J. Volk, V. Avrutin, H. Morkoc, Ü. Ozgür, J Appl Phys 119, 095311 (2016); <https://doi.org/10.1063/1.4942835>
- [22] F.Z. Bouchereb, memoire de magister, universited'Oran (2014).
- [23] Y.Z. Zhu, G.D. Chen, Ye Honggang, A. Walsh, C.Y. Moon, W. Su-Huai, alloysPhys Rev B 77, 245209 (2008); <https://doi.org/10.1103/PhysRevB.77.245209>
- [24] A. Djelal, K. Chaibi, N. Tari, K. Zitouni, A. Kadri, Superlattices and Microstructures 109, 81 (2017); <https://doi.org/10.1016/j.spmi.2017.04.041>
- [25] S. Limpijumnong, W.R.L. Lambrecht, Phys. RevB 63, 104103 (2001);
<https://doi.org/10.1103/PhysRevB.63.104103>
- [26] S. Kazuhiro, T. Naomichi, N. Yoshiaki, H. Tomoyasu, K. Hitoshi, Phys Rev B 88, 075203 (2013).
- [27] F. Daniel, J.M Benjamin, W. Aron, Nanoscale Research Letters 12, 1779 (2017).
- [28] S. Labidi, J. Zeroual, M. Labidi, K. Klaa, R. Bensalem, Solid State Phenomena 257, 123 (2017); <https://doi.org/10.4028/www.scientific.net/SSP.257.123>
- [29] M. Dadsetani, R. Beiranvand, J Solid State Sci 11, 2099 (2009);
<https://doi.org/10.1016/j.solidstatesciences.2009.08.018>
- [30] H. Baltache, R. Khenata, M. Sahnoun, M. Driz, B. Abbar, B. Bouhafs, Physica B 344, 334 (2004); <https://doi.org/10.1016/j.physb.2003.09.274>
- [31] M. Brik, Journal of Physics Condensed Matter 25, 345802 (2013);
<https://doi.org/10.1088/0953-8984/25/34/345802>